Structural and Rheological Properties of Meibomian Lipid

Liat Rosenfeld,[1] Colin Cerretani,[2] Danielle L. Leiske,[1] Michael F. Toney,[3] Clayton J. Radke,[2,4] and Gerald G. Fuller[1]

[1]Department of Chemical Engineering, Stanford University, Stanford, California
[2]Department of Chemical and Biomolecular Engineering, University of California, Berkeley, Berkeley, California
[3]Stanford Synchrotron Radiation Lightsource, Stanford Linear Accelerator National Accelerator Laboratory, Menlo Park, California
[4]Vision Science Group, University of California, Berkeley, Berkeley, California

Correspondence: Gerald G. Fuller, Department of Chemical Engineering, Stanford University, Keck 183, Stanford, CA, 94305-5025; ggf@stanford.edu.

Submitted: September 18, 2012
Accepted: March 2, 2013

Citation: Rosenfeld L, Cerretani C, Leiske DL, Toney MF, Radke CJ, Fuller GG. Structural and rheological properties of meibomian lipid. *Invest Ophthalmol Vis Sci.* 2013;54:2720–2732. DOI:10.1167/iovs.12–10987

Purpose. We explore the unique rheological and structural properties of human and bovine meibomian lipids to provide insight into the physical behavior of the human tear-film lipid layer (TFLL).

Methods. Bulk rheological properties of pooled meibomian lipids were measured by a commercial stress-controlled rheometer; a home-built interfacial stress rheometer (ISR) probed the interfacial viscoelasticity of spread layers of meibomian lipids. Small- and wide-angle x-ray scattering detected the presence and melting of dispersed crystal structures. Microscope examination under cross polarizers provided confirmation of ordered crystals. A differential scanning calorimeter (DSC) analyzed phase transitions in bulk samples of bovine meibum.

Results. Bulk and interfacial rheology measurements show that meibum is extremely viscous and highly elastic. It is also a non-Newtonian, shear-thinning fluid. Small- and wide-angle x-ray diffraction (SAXS and WAXS), as well as differential scanning calorimetry (DSC) and polarizing microscopy, confirm the presence of suspended lamellar-crystal structures at physiologic temperature.

Conclusions. We studied meibum architecture and its relation to bulk and interfacial rheology. Bovine and human meibomian lipids exhibit similar physical properties. From all structural probes utilized, we find a melt transition near eye temperature at which lamellar crystals liquefy. Our proposed structure for the tear-film lipid layer at physiologic temperature is a highly viscoelastic, shear-thinning liquid suspension consisting of lipid lamellar-crystallite particulates immersed in a continuous liquid phase with no long-range order. When spread over on-eye tear, the TFLL is a duplex film that exhibits bulk liquid properties and two separate interfaces, air/lipid and water/lipid, with aqueous protein and surfactantlike lipids adsorbed at the water/lipid surface.

Keywords: meibomian lipids, rheological properties, structural properties

Meibomian lipids are the major component of the tear-film lipid layer (TFLL), the outermost portion of the tear film. Between the lipid layer and the corneal surface exists a 3- to 10-μm aqueous layer[1] containing salts, mucins, and proteins. The primary role of the aqueous tear film is to hydrate and protect the corneal surface. The lipid layer, estimated to be approximately 100-nm thick,[1,2] is a duplex film that spreads over the aqueous tear film after each blink. It is thought to reduce evaporation from the aqueous phase and to play an important role in maintaining tear-film stability.[2,3] Tear-film instability and increased tear evaporation are major signs of dry-eye disease, an ocular surface disease that leads to discomfort and possible damage to the corneal and conjunctival epithelia.[4] Since the physical and mechanical properties of the TFLL depend on the structure of meibum, knowledge of meibum's structure is indispensable to understand the function of the TFLL in tear-film behavior.

Produced in the meibomian glands, meibum is a holocrine secretion composed of a rich mixture of lipids and possibly cellular debris. Wax esters and cholesterol esters are the major lipid components, together making up roughly 60% to 70% of the total meibum content, with lesser amounts of diesters, triacylglycerols, polar lipids, and fatty acids making up the balance. Many of the individual chains are longer than 20 carbons, leaving lipids with one or more alkyl chains, such as wax esters, diesters, and triacylglycerols, to contain as many as 40 to 60 carbon atoms. The degree of saturation varies as well: saturated, monounsaturated, and polyunsaturated lipids are all present in meibum.[5–8] Meibomian-gland secretions have also been shown to contain proteins, which could disrupt regions of ordered lipids.[9,10]

To date, most efforts at characterizing meibum have focused on chemical analysis of the secretion. Less is known about the structure and physical properties of meibum. Various authors found that meibum exhibits a broad melting range, becoming liquid near body temperature.[11] Viscosity measurements by Tiffany and Dart[12] demonstrated meibum to be viscous, although the effects of shear rate or temperature were not pursued. Borchman et al.[13] used infrared spectroscopy to characterize the molecular conformation of hydrocarbon chains in human meibum, finding that as meibum melts, hydrocarbon chains of the lipids transition from the *trans* to *gauche*

rotomers. The increased disorder reduces the packing efficiency of the lipids. By using small-angle x-ray scattering (SAXS), Leiske et al.[14] observed crystalline structures in bulk human meibum. Two crystal populations were present, one melting at 34°C and another persisting up to 40°C. They also measured rheology of interfacial meibum films spread on water and found that the film undergoes a sharp phase transition from solidlike to liquidlike behavior below physiological temperature.

A major reason for the scarcity of information about meibum is the difficulty in obtaining large enough human samples for making measurements. Consequently, researchers often use other mammals as a source of meibum.[15–17] Nicolaides et al.[16,17] studied the lipid composition of both steer and human meibum and found them to be similar.

In this work, we explore the bulk and interfacial properties of human and bovine meibum in an effort to understand how its structure relates to its physical properties. We explore temperature-induced transitions in the structure and mechanical properties of these meibomian lipids. Using SAXS, we detect the presence of crystal structures and observe their melt behavior. In addition, differential scanning calorimetry provides temperatures at which phase changes occur and their corresponding latent heats. We perform interfacial and bulk rheology measurements to probe how thin films and bulk samples of meibum respond to deformation over a range of shear rates and temperatures. By comparing the behavior of dispersed crystal structures to the measured mechanical properties over a range of temperatures, we gain understanding of how meibum's molecular organization contributes to its physical behavior.

Methods

Meibomian Lipid Collection

Animal and human ethics were approved for the collection of meibomian lipids; the study was carried out in accordance with the tenets of the Declaration of Helsinki. Bovine eyelids of more than 200 animals were dissected postmortem at a slaughterhouse. The eyelids were warmed to 37°C, and the meibomian lipids were extruded by hard expression of the superior and inferior eyelid margins[16,17] with pliers, yielding an average of 3 mg per eye. The excreta were scraped from the lid margin with a metal spatula and deposited onto a small glass cover slip that was then placed in an amber jar for storage at −20°C until use. The excreted fluid was a clear liquid at 37°C, and became opaque and yellowish upon solidification at room temperature. The bulk rheological experiments required pooling of bovine meibum from multiple animals to generate samples large enough for analysis. Otherwise, samples from individual animals were stored and tested separately.

Twelve human-meibum samples, each less than 1 mg (i.e., five samples of 0.3–0.5 mg, four samples at 0.6–0.8 mg, and three samples between 0.8–1.0 mg), were collected from healthy, non–dry-eye, non–lens-wearing volunteers. A meibum sample was collected only when, on examination, the volunteer met the following criteria: lack of dry eye symptoms (<5) as determined by the Schein Questionnaire[18]; minimal to absence of sodium fluorescein staining in the cornea; tear-film break-up time longer than 7 seconds; and absence of meibomian gland dysfunction (MGD) as determined by normal meibum appearance.

Meibum was expressed from the lower lids by applying pressure with a sterile cotton swab against a Mastrota paddle (Medi Instrument Inc., New York, NY). Gentle scraping of the eyelid margin with a small, degreased metal ocular spud collected secreted meibum. Samples collected from the right and left eyes of a single volunteer were pooled and transferred onto a small glass cover slip that was then placed in an amber jar. Collected samples were packed in dry ice, shipped overnight, and stored upon arrival at −20°C until use. Here too, the bulk rheological experiments required pooling samples from four individuals.

Interfacial Shear Rheometry

An interfacial stress rheometer (ISR) probed the interfacial viscoelasticity of the meibomian lipids. Validation and merits of this technique are available elsewhere.[19,20] Briefly, the ISR is a two-dimensional analogue to a classic, three-dimensional sliding-plate rheometer. It ascertains the viscoelastic properties of monolayers. Our ISR uses a KSV mini-trough (KSV NIMA/Biolin Scientific, Espoo, Finland) coupled with a Wilhelmy balance (KSV NIMA/Biolin Scientific) and moveable barriers to monitor and control surface pressure. Two Helmholtz coils apply an oscillating magnetic field used to move the magnetic, Teflon-coated rod along its major axis at sinusoidal strains. The rod floats at the interface in a rectangular, quartz channel. The long axis of the channel is perpendicular to the trough barriers so that compression of the monolayer throughout the trough (inside and outside the channel) is uniform. The channel maintains the lateral position of the rod during the experiments and defines the velocity profile created by the rod motion. Resulting stress was calculated from a calibration constant that converted the strength of the magnetic field to the force (the rheometer was calibrated prior to deposition of every monolayer). Rod position was monitored with a charge-coupled device camera (Basler Electric Company, Highland, IL) and strain was ascertained from the images. The trough surface was heated to 35°C to facilitate sample spreading. Solid meibum touched to the trough surface with a metal spatula spread spontaneously. To ensure reproducible measurements, each sample was first spread to a constant surface pressure of 2 mN/m. After spreading, the trough was cooled to 20°C over a period of 1 hour before the film was compressed to the desired surface pressure. Trough surface area was held constant as the interface was slowly heated to 35°C at 0.3°C/min. During the heating cycle, interfacial rheology was monitored at a frequency of 1 Hz and a strain of 1.74%, which is within the linear viscoelastic region of meibum. Temperature changes in time were monitored by placing a temperature probe 1 to 2 mm below the surface behind the trough barriers.

Recent Brewster Angle Microscopy (BAM) measurements[15] showed that on deposition, meibomian lipids spread from solvent are inhomogeneous. At 15 mN/m and above, the surface pressure at which the elasticity of the film increased, and the film was homogeneous on length scales as small as the limit of BAM. These measurements reveal surface microstructures on the order of at most 100 μm, a much smaller length scale than that of the ISR gap width.

Bulk Shear Rheometry

Shear rheology of pooled bovine meibomian lipids was measured using a stress-controlled rheometer (Model AR G2; TA Instruments, New Castle, DE) with an 8-mm parallel plate and a gap size of 250 μm. Due to the small volume of an individual human-meibum sample (of the order of 0.3 μL), shear rheology of four pooled human-meibomian samples was measured with a 3-mm parallel plate and a gap size of 100 μm. Samples were loaded at 23°C. Both steady shear rheology and oscillatory shear rheology were performed on every sample. For oscillatory rheological measurements, a stress sweep was first performed to obtain the linear viscoelastic region. Then

the sample was heated at a constant rate of 1°C per minute while oscillating the upper plate at 1 Hz and 0.1% strain, which is within the linear viscoelastic region for the sample.

SAXS

SAXS experiments were performed at the Stanford Synchrotron Radiation Lightsource (SSRL) on beamline 1 to 4. Bovine-meibum samples were sandwiched between two Kapton windows (Kapton Source, Monrovia, CA) in a sample holder. A two-dimensional detector collected scattering intensity *I(q)* over 2-minute intervals for the combined sample and holder. Scattering of the empty sample holder with Kapton windows (Kapton Source) was also recorded. Transmission of the holder and sample were measured to normalize intensity and remove scattering volume dependence; an empty cell was subtracted as the parasitic scattering. Background (diffuse) scattering was removed, and a function was fit to the baseline and subtracted from the data, ensuring that the background was independent of the scattering vector, q [Å^{-1}], which for ordered structures is related to length scales in real space, d [Å], by the expression: $q = 2\pi/d$. Scattering peaks were fit with Gaussian functions to determine peak centers and widths. Scattering spectra of the samples were measured at temperature increments of 3 to 4°C between 26 and 45°C. Samples were heated until the peaks disappeared; therefore, not all samples were heated to 45°C.

Wide-Angle X-Ray Scattering

Wide-angle x-ray scattering (WAXS) experiments were also performed at SSRL beamline 1 to 4. The technique was the same as that for SAXS. However, the distance between the sample and the detector was shorter, and, thus, diffraction maxima at larger angles were observed.

Polarized-Light Microscopy

Micrographs of bovine meibum were obtained with a polarized-light microscope (Olympus BX51; Olympus, Tokyo, Japan) attached to a color digital camera (Olympus C-5060; Olympus). A sample from a single animal was sandwiched between a glass slide and a cover slip, placed on a temperature-controlled stage, and subjected to temperature cycling between 15 and 150°C at a rate of 2°C per minute with still images (1024 × 768 pixels) captured every 30 seconds. Two polarizing filters were oriented 90° to each other: one between the light source and the sample, and one between the sample and the camera (Olympus C-5060; Olympus). Birefringence due to anisotropic crystal structures was evident in the visible bright areas of the images.

To quantify birefringence intensity, images were converted to grayscale, and the average intensity, I, of all image pixels (~8×10^5 pixels) was calculated. We define a relative intensity, I/I_{max}, where I_{max} corresponds to the average pixel intensity of the brightest image. To ascertain melting or crystallization transitions, we tracked I/I_{max} versus temperature.

Differential Scanning Calorimetry

A TA Instruments differential scanning calorimeter (DSC) (Model DSC Q20; TA Instruments, New Castle, DE) was used to analyze phase transitions in bulk samples of bovine meibum. At temperatures in which phase transitions occur, latent heat is absorbed or released, resulting in a peak in heat inflow or outflow at that temperature. Peak location and width reveal the temperature ranges for a particular phase transition; integration of the peak gives the total latent heat released or absorbed for a given phase transition; 5- to 10-mg individual and pooled samples of bovine meibum taken from storage at −20°C were hermetically sealed into aluminum TA-Tzero sample pans (TA Instruments). Carefully sealed samples were then placed in the DSC holder, and temperature was cycled between −30 and 200°C at a rate of 2°C per minute for at least two complete cycles. Peak areas were quantified with the TA Analysis software (TA Instruments). We subjected 11 samples of bovine meibum to a combined 25 heating/cooling cycles.

Results

Interfacial Shear Rheology

The change in bovine-meibum interfacial viscoelastic properties as the film was heated or cooled is presented in Figure 1. *G'* stands for the elastic modulus while *G"* stands for the viscous modulus. The SD of six measurements was ±5% for both heating and cooling and is within the size of the data points. At 23°C and a surface pressure of 24 mN/m, the film was quite elastic (*G' > G"*) with high values, near 10 mN/m. As the film was heated, the interfacial moduli decreased by almost three orders of magnitude. Between 29 and 31°C, the interfacial elastic modulus dropped most rapidly; the film became primarily viscous (*G" > G'*) at approximately 30°C. At 35°C,

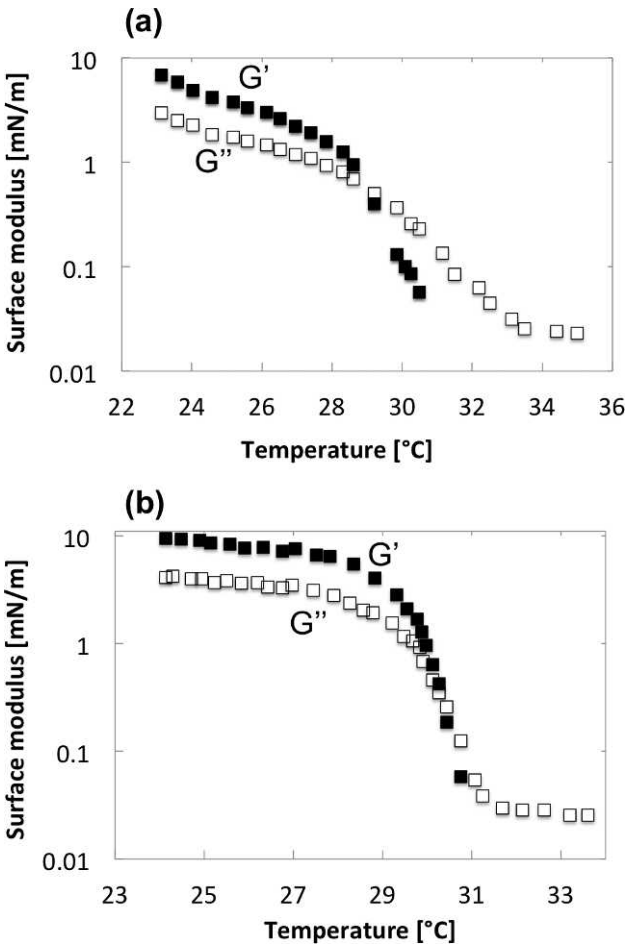

Figure 1. Interfacial moduli as a function of temperature for a representative bovine-meibomian lipid film at a frequency of 1 Hz and a strain of 1.74%. The film was initially compressed to 24 mN/m at 23°C, then the surface area was held constant as the film was heated to 35°C (**a**), and then cooled back to 23°C (**b**). *Filled symbols* represent the elastic modulus, *G'*, and *open symbols* represent the viscous modulus, *G"*. *Error bars* are within the size of data points.

the interfacial viscous modulus was at the sensitivity limit for the ISR (0.02 mN/m). After reaching 35°C, the film was cooled back to 23°C (Fig. 1b). Over the temperature range, 35 to 31°C, the film was viscous with no measureable elastic component. An interfacial elastic modulus was discernible at 31°C and rose very quickly between 31 and 29°C. The film became primarily elastic at 29°C. Comparison between the two curves reveals a sharper transition when the film is cooled; the film becomes rigid over a very narrow temperature range. Moreover, the values of both the interfacial elastic and viscous moduli are higher at the base temperature (23°C) after heating and then cooling.

Bulk Shear Rheology

The bulk viscoelastic properties obtained from oscillatory shear rheology of pooled samples are presented in Figure 2 for bovine meibum and in Figure 3 for human meibum. The elastic (*G'*) and viscous (*G"*) moduli are shown as functions of temperature. Temperature sweeps from 25 to 40°C and 40 to 25°C were performed as presented in Figures 2a, 2b for bovine meibum and in Figures 3a, 3b for human meibum. For the bovine meibum, the major melt transition occurred between 29 and 35°C. In that 6°C temperature range, the viscous and elastic moduli both decreased by three orders of magnitude during heating. Despite the dramatic decrease in viscoelasticity, the fluid remains predominantly elastic (*G' > G"*). Comparison of the two curves reveals that the transition during cooling is sharper than that during heating. Moreover, the temperature range in which the transition occurs, 32 to 36°C, is higher in the cooling process than in the heating process, 27 to 35°C. The SD of five measurements was less than 4%, too small to be shown in the figures.

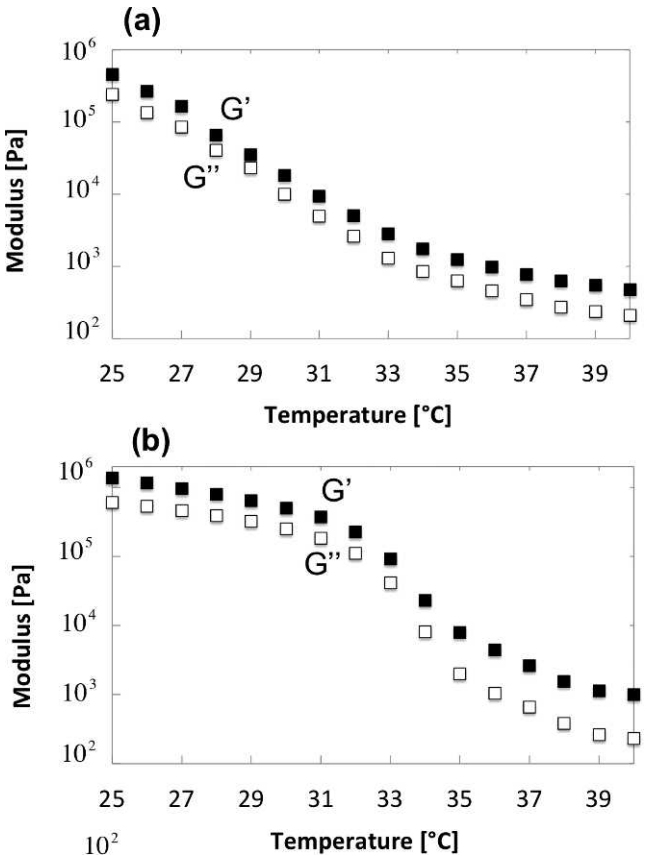

FIGURE 2. Bulk moduli as a function of temperature for pooled bovine-meibomian lipid. The sample was loaded at 25°C and heated to 40°C (**a**) and cooled back to 25°C (**b**). *Filled symbols* represent the elastic modulus, *G'*, and *open symbols* represent the viscous modulus, *G"*. *Error bars* are within the size of data points.

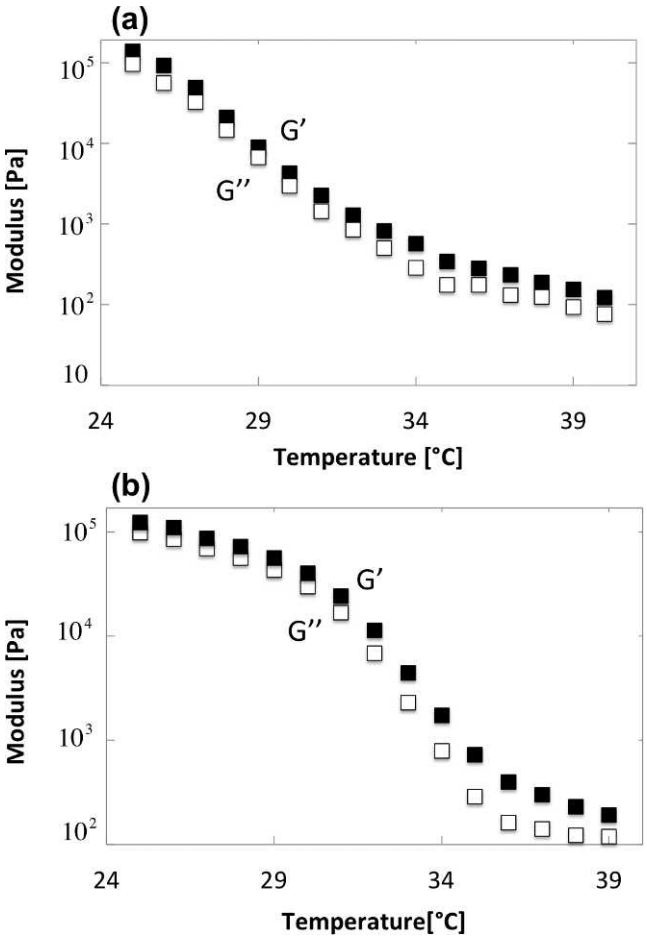

FIGURE 3. Bulk moduli as a function of temperature for pooled human-meibomian lipid. The sample was loaded at 25°C and heated to 40°C (**a**) and cooled back to 25°C (**b**). *Filled symbols* represents the elastic modulus, *G'*, and *open symbols* represent the viscous modulus, *G"*. *Error bars* are within the size of the data points.

The human-meibum shear rheology in Figure 3 displays the same general behavior as that for the bovine meibum. Here too, a phase transition is observed between 29 and 35°C where the viscous and elastic moduli both decrease by three orders of magnitude. The maximum magnitude of the viscous and elastic moduli is lower than that of bovine meibum but within the same order of magnitude. Likewise, the SD of three measurements was ±3.67%.

Additional temperature sweeps for bovine meibum were performed from 25 to 150°C and back to 25°C to reveal the temperature at which the fluid becomes purely viscous (the point at which the elastic modulus cannot be detected). Results are presented in Figure 4. They show that the fluid is mostly elastic even at very high temperatures. Only above 140°C does the fluid become more viscous than elastic. In human meibum, measurements were not performed at temperatures higher than 40°C due to the small sample size and the difficulty in obtaining signal at high temperature. SD over three measurements was ±1.84% to 3.14%.

The bulk viscosity of meibum as a function of shear rate at various temperatures is presented on log-log scales in Figure 5 for bovine meibum and in Figure 6 for human meibum. SD of the measured viscosities over three repeated samples was less

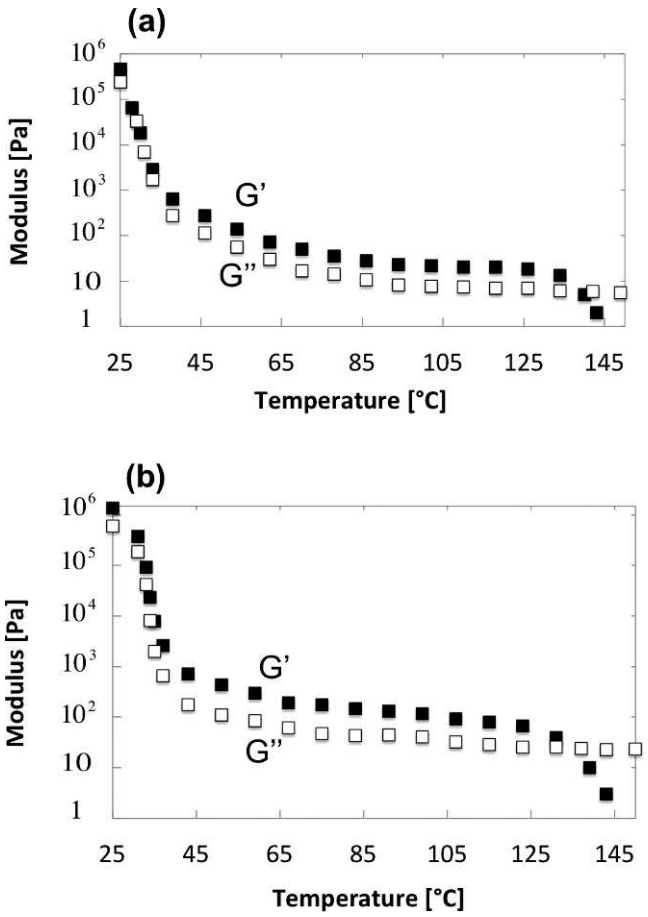

FIGURE 4. Bulk moduli as a function of temperature for pooled bovine-meibomian lipid. The sample was loaded at 25°C and heated to 150°C (**a**) and cooled back to 25°C (**b**). *Filled symbols* represents the elastic modulus, *G'*, and *open symbols* represent the viscous modulus, *G"*. *Error bars* are within the size of data points.

than 5%. Bovine-meibum viscosity is very large, approximately 10^5 times more viscous than water at 35°C. It decreases with shear rate even up to 150°C where the elastic modulus is undetectable. Human-meibum shear viscosity likewise decreases with increasing shear rate. Hence, human and bovine meibum are non-Newtonian even when the viscous modulus dominates the elastic modulus.

SAXS

SAXS spectra of bovine meibum were recorded for 10 individual-animal samples at five temperatures between 27 and 40°C. A representative diffraction pattern is shown in Figure 7. Several peaks are detected at different scattering vectors, q. All samples contained at least three lipid phases. Peak A, which has first- and second-order peaks at q of 0.122 ± 0.002 $Å^{-1}$ and 0.244 ± 0.003 $Å^{-1}$ (average ± SD of 10 samples), corresponds to a lamellar packing of 51.24 ± 0.54 Å. Peak B, which has first- and second-order peaks at q of 0.062 ± 0.02 $Å^{-1}$ and 0.124 ± 0.01 $Å^{-1}$, corresponds to a lamellar packing of 101.6 ± 0.78 Å. The fact that we observe two peaks with peak q ratios of 2:1 shows that the scattering originates from lamellar-ordered phases. Peak C at q of 0.164 ± 0.025 $Å^{-1}$ corresponds to a packing of 40.27 ± 0.51 Å, and peak D at q of 0.272 ± 0.015 $Å^{-1}$ corresponds to a packing of 23.1 ± 0.46 Å. Peaks A, B, and C were detected in all 10 samples. Peak D was detected in 5 of 10 samples. Phase A, corresponding to peak A, is referred to as the majority crystallite phase, since its measured intensity is the largest. The temperature dependence of each peak's maximum intensity was extrapolated linearly to zero intensity to reveal the melt temperature. The average melt temperature of the majority crystalline phase (phase A) is 37.4°C (Fig. 8a). Phase B, with longer lamellar spacing, melted at a lower temperature, 34.3°C, than that of phase A (Fig. 8b). The two other lamellar phases, C and D, melted at 36.1 and 36.3°C, respectively. Because peaks C and D melt at the same temperature, we believe that they are from the same lamellar phase. In fact, the five samples in which peak D did not appear had lower intensities than the other five samples. Because the intensity of peak D is weaker than that of peak C, it is not detected when the total intensity from the sample is weak.

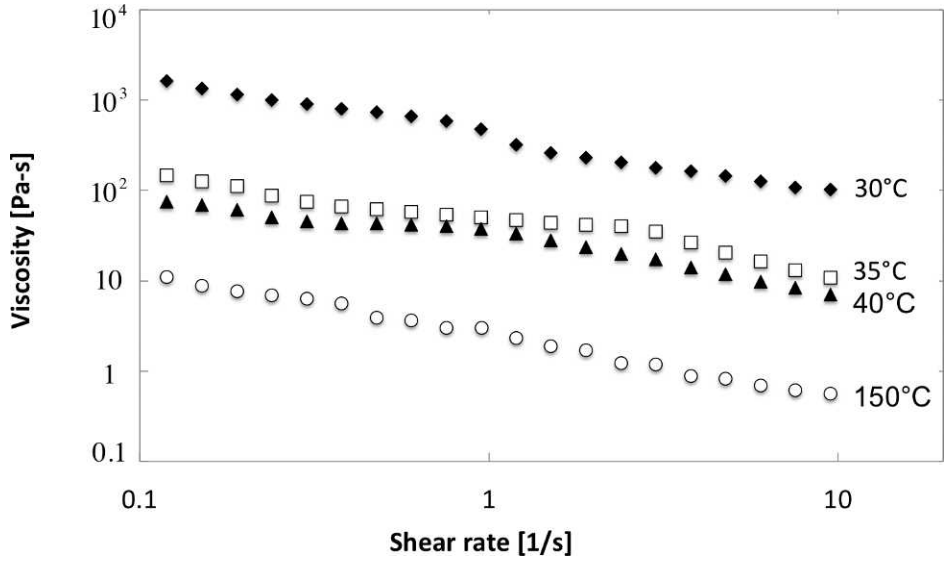

FIGURE 5. Bovine-meibum bulk viscosity as a function of shear rate for various temperatures. *Error bars* are within the size of data points.

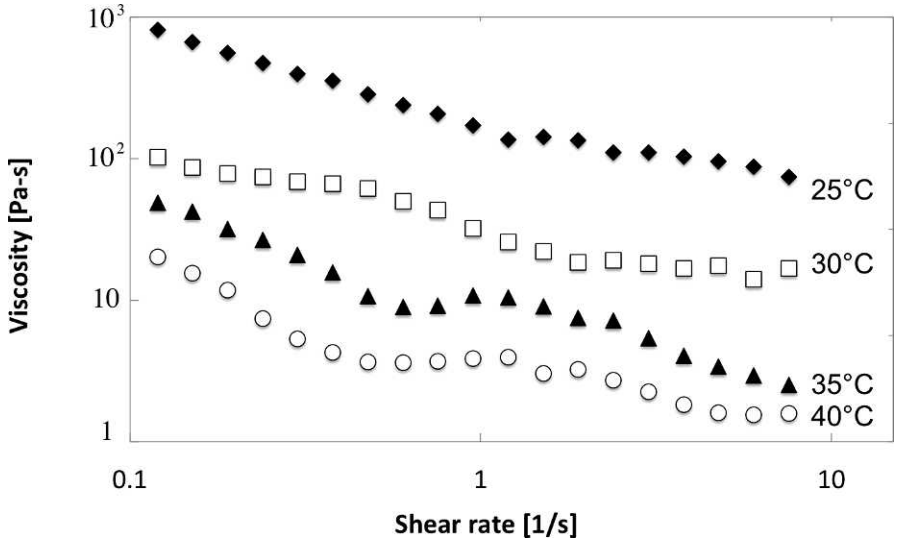

FIGURE 6. Human-meibum bulk viscosity as a function of shear rate for various temperatures. *Error bars* are within the size of data points.

WAXS

WAXS spectra were recorded for five individual-animal samples at 11 temperatures between 27 and 145°C. As illustrated in Figure 9, two broad peaks were detected in all samples. Peak E at q of 1.52 ± 0.002 Å^{-1} corresponds to a lamellar packing of 4.13 ± 0.03 Å and peak F at q of 1.35 ± 0.001 Å^{-1} corresponds to a lamellar packing of 4.64 ± 0.02 Å. With increasing temperature, the phase represented by peak E melts into phase F, raising the intensity of peak F until peak E completely disappears at 34.34 ± 0.30°C. Because the melt temperatures for WAXS peak E and SAXS peak B in Figure 7 are the same, these peaks likely reflect the same material. SAXS peak B corresponds to the lamellar spacing in phase B, whereas WAXS peak E corresponds to the lateral spacing of the polar head groups in this crystalline phase. Due to crystallite melting, peak F slowly disappears between 36 and 145°C. Even at 145°C, however, traces of peak F were detected. The width of peak F was much greater than that of peak E, indicating that peak F represents a maximum intensity of the combined E and F peaks. The temperature dependence of peak E and that of E and F combined is shown in Figure 10.

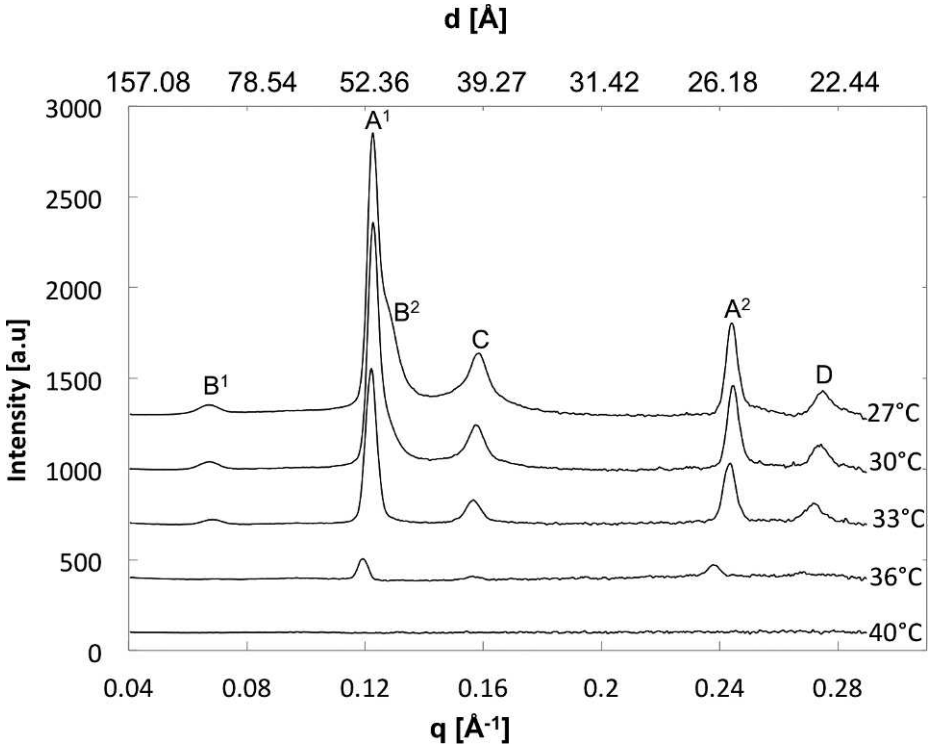

FIGURE 7. SAXS diffraction spectra of bovine meibum containing crystalline structures. Scattering at multiple temperatures between 27 and 40°C is shown. Peaks representing unique phases are lettered *A*, *B*, *C*, and *D*, and the *superscripts* above the peak labels denote the order of the peak (first-second).

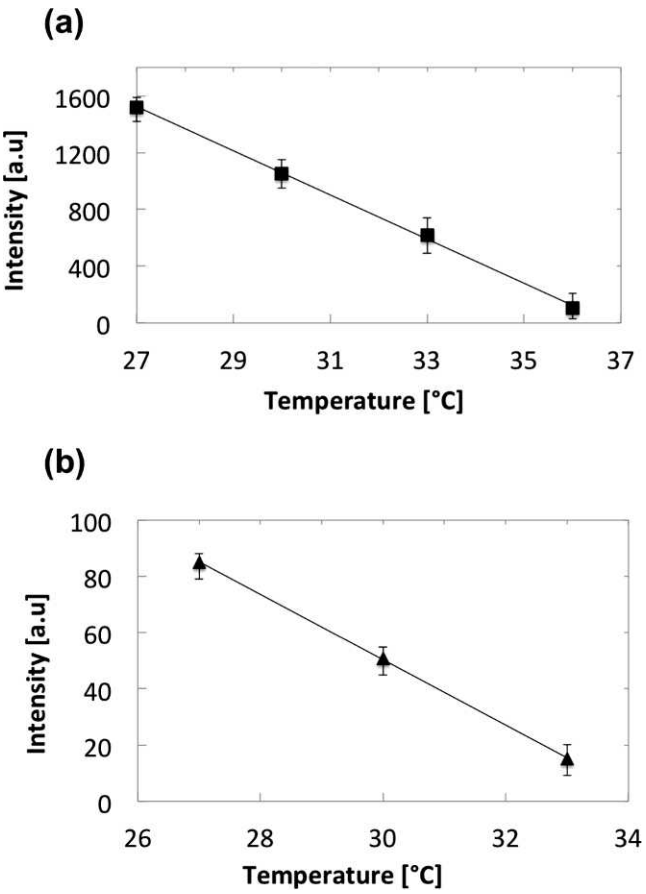

FIGURE 8. (**a**) Maximum intensity of peak A in Figure 7 as a function of temperature with an SD of 10 samples. The melt temperature for this peak is 37.4°C. (**b**) Maximum intensity of peak B in Figure 7 as a function of temperature with an SD of 10 samples. The melt temperature for this peak is 34.3°C. The intensity of both peaks decreases linearly with temperature as the crystallites melt.

Polarized-Light Microscopy

Micrographs of bovine meibum viewed through cross-polarized light are composed of dark areas indicating isotropic fluid and bright areas corresponding to optically anisotropic crystal structures. Figure 11 gives an I/I_{max} melting curve for a sample of bovine meibum, where I_{max} corresponds to the average brightness of the image at 30°C. As the temperature increases at 2°C per minute from 30°C, I/I_{max} decreases because anisotropic crystallites melt. By approximately 36 to 37°C, almost all birefringent crystalline material has melted; I/I_{max} asymptotes with further increases in temperature. Samples imaged at temperatures above 37°C are essentially black with almost no visible features. Upon further heating to 150°C, no changes are seen in the cross-polarized images.

Differential Scanning Calorimetry

We subjected bovine meibum to differential scanning calorimetry. Two of the meibum samples were from individual animals, and the rest consisted of pooled meibum from multiple animals. There was no qualitative difference between the two sets of samples. Figure 12 is a typical heating/cooling scanning curve. Starting at −30°C, the sample is slowly heated and an endothermic peak occurs at 0 ± 2°C (mean ± SD). A second broader peak appears between 20 and 35°C with a maximum at 30.7 ± 1.1°C corresponding to melting of crystalline meibum, as seen in the SAXS spectra of Figure 7. Near 100°C, several close endothermic peaks appear, followed by a larger one near 125°C (123.5 ± 1.2°C). Upon cooling from 200°C, no corresponding high-temperature exothermic peaks appear, but a freezing transition is detected between 35 and 20°C with a maximum at 27.8 ± 2.3°C. Reheating of the sample from −30 to 200°C results only in the broad melting peak near 30°C. The 0°C, 100°C, and 125°C peaks all disappear after the first heating cycle.

Some meibum samples were first dried in a desiccator for 2 days at ambient temperature and then scanned as above. Results were similar to those in Figure 12, with the notable absence of both the 0°C and high-temperature peaks. Subsequently, meibum samples were hydrated in the desiccating chamber at approximately 90% relative humidity for 4 days. DSC scans demonstrate the reappearance of the peaks at 0 and 100°C, but not that at 125°C. If we divide the area under the 0°C and 100°C peaks by the enthalpy of water freezing and vaporization, respectively, the corresponding amount of water in the meibum samples ranges from 1 to 4 wt%.

DISCUSSION

Extensive effort is available on the chemical composition of human meibum.[2,5–8,10,11,16,17,21–24] By comparison, surprisingly little is known about the physical structure of the TFLL and how that structure influences on-eye behavior. Most proposed structures are similar to the sketch of McCulley and Shine[23,25] shown in Figure 13. Here the more polar lipids orient vertically at the water/lipid interface akin to surfactants at an oil/water interface. Less-polar lipids organize into several lamellar layers with the least-polar hydrocarbons vertically oriented at the air/lipid interface. If we assume a typical length of 2.5 nm for a lipid molecule and accept Figure 13 literally, the thickness of the lipid layer is less than approximately 10 nm. In contrast to the accumulation of detailed information on the chemical composition of human meibum, the basic lamellar structure suggested by Figure 13 remains[8,26] (see, for example, Fig. 1 of the Meibomian Gland Dysfunction report[8]). The one change in structure now made explicit is that proteins adsorb at the lipid/water interface and possibly intercalate into the remaining lipid layers (see Refs. 2, 8, and 27 and Millar TJ and Mudgil P. *IOVS* 2005;46:ARVO E-Abstract 4418). A recently proposed TFLL architecture better illustrates the duplex-film thickness of the film, but does not address the physical structure of the lipids within that film.[28] Our proposed picture of the human TFLL contrasts strongly[28] and also with that of McCulley and Shine[23,25] (Fig. 13).

Early evidence of the lipid-layer thickness cited interference color patterns observed under white light,[29–35] which demands thicknesses near 100 nm. The more in-depth studies of King-Smith et al.[36] using in situ interferometry, suggest lipid-layer thicknesses between 20 and 160 nm. Even at the smallest cited thickness of 20 nm, the lipid layer is not well represented by a monolayer, but rather by 6 to 10 multilayers. At this thickness, the TFLL is best viewed as a duplex film (i.e., an oily layer that is thick enough to exhibit bulk properties with two distinct interfaces).[37,38] In this scenario, also suggested by Holly,[39,40] the tear-film lipid layer consists of two separate interfaces: air/lipid and water/lipid separated by bulk liquid. A stack of vertically oriented lamellae extending across the entire film is an unlikely bulk structure, as it demands an almost a rigid solid (Bron AJ, et al. *IOVS* 2011;52:ARVO E-Abstract 3854). Also, a lamellar-stack structure disagrees with the discrete melting behavior found in our rheologic, scattering, and DSC experiments. As with most duplex films spread at the air/water interface, breakup into nonuniform regions is likely for the

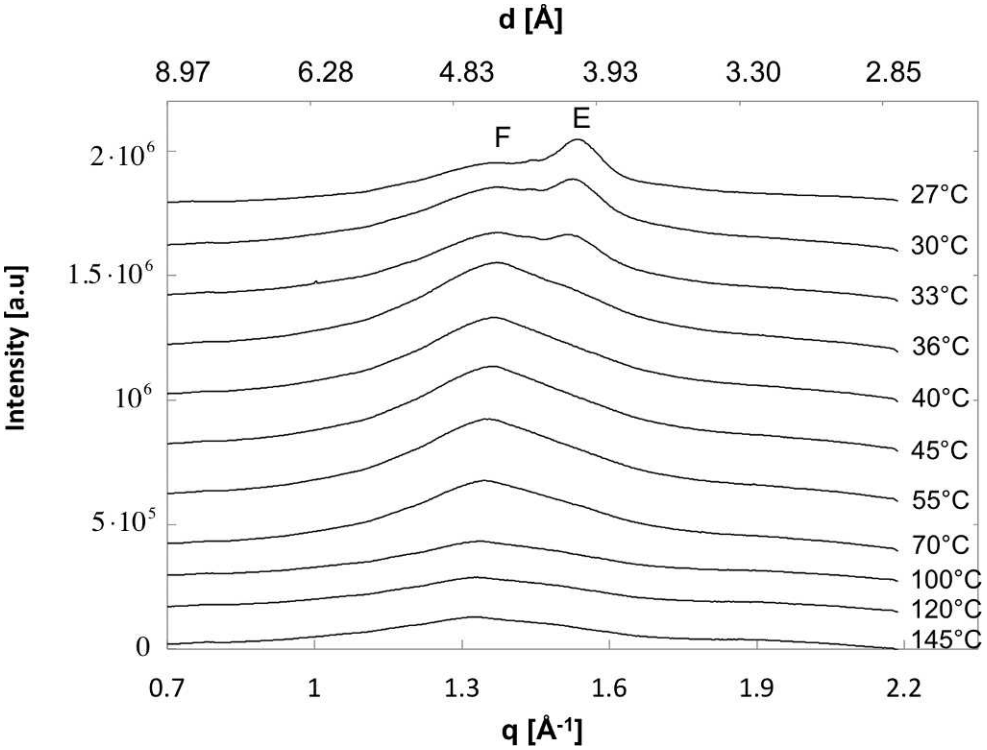

FIGURE 9. WAXS diffraction patterns of a representative bovine-meibomian lipid containing crystalline structures. Scattering at multiple temperatures between 27 and 145°C is shown.

thinner lipid layers, as has been observed both in vitro and in vivo for tear-film lipid layers.[41,42] Lipid-layer breakup, however, is not anticipated in the thicker regions of the rising lipid curtain during initial spreading.

To provide a more complete description of the TFLL, we explored interfacial and bulk rheological and scattering properties of meibum. Because of sample availability, we focused primarily, although not exclusively, on bovine meibum. In addition to compositional similarity with human meibum,[16] our experiments show that bovine meibum is both rheologically and structurally similar to human meibum.[14] To within minimal differences, bovine meibum is a useful physical model for human meibum.

Surprisingly few studies are available on the bulk rheology of human meibum. The previous effort of Tiffany and Dart[12] was semiquantitative and did not examine the roles of shear rate or temperature. More recently, Yokoi et al.[43] analyzed the rise kinetics of the human lipid layer after a blink. Based on a simplified analysis, they concluded that the TFLL is elastic and that it drags the underlying viscous tear film upward as it spreads. Thus, the entire tear film (i.e., tear film plus lipid layer) behaves as if viscoelastic. In our study, the bulk and interfacial rheology are examined over a range of temperatures, oscillatory frequencies, and shear rates. We find that bulk meibum is both viscous and elastic. At 35°C, the shear viscosity of bovine and human meibum is approximately 10^5 larger than that of water. Likewise, bulk meibum is strongly shear thinning even at temperatures up to 150°C. The large viscosity and dramatic shear thinning indicate that bulk meibum is structured and inhomogeneous.

Bovine and human meibum are also highly elastic with elastic moduli even larger than their viscous moduli. The viscous and elastic moduli of bovine and human meibum are approximately 10^2 to 10^3 Pa at 35°C at 1 Hz. In comparison, typical soft contact lens materials have moduli approximately 10^6 Pa.[44] Oscillatory rheology shows that meibum remains primarily elastic until 140°C. This observation is further confirmation of fluid structure even at high temperature. Both steady and oscillatory shear rheology demonstrate a dramatic decline in both meibum viscosity and storage and loss of moduli between 30 and 36°C, suggesting the presence and subsequent melting of crystalline material over that temperature range.

Interfacial rheological properties of the bovine- and human-meibomian lipids also show that meibum is viscoelastic at room temperature. Similar to bulk meibum, the interfacial elastic modulus below 30°C is larger than the interfacial viscous modulus. The observed enhancement of the elastic and viscous moduli at 23°C after heating and cooling corresponds with the observation by Mudgil and Millar,[45] who reported that cooling enhances the surfactant properties of meibomian lipids. Again, similar to bulk meibum, there is a melting transition near 30°C at which both interfacial moduli diminish dramatically. Thus, bulk and interfacial rheology indicate that meibum is viscoelastic and that at ambient temperature, crystalline material is present that partially melts near eye temperature. Surprisingly, the fully melted material above 40°C remains viscoelastic even to high temperature.

X-ray scattering from human and bovine meibum is consonant with the rheological characterization. SAXS spectra demonstrate the presence of lamellar crystalline structures in bulk meibum. One crystal population melts by 34°C, two more by 36°C, and the majority crystalline phase by 37°C. At bovine ocular-surface temperature[46] of approximately 34 to 38°C, as many as three crystal populations are present. SAXS diffraction of bovine meibum differs only slightly from that of humans.[14] Grazing-incidence x-ray diffraction measurements of human meibum by Leiske et al.[47] show the presence of crystalline lamellar regions of lipid even in films only several molecular layers thick spread over water. Based on the similarity between the bulk structure of bovine and human meibum as demonstrated by SAXS and WAXS, we expect multimolecular films of

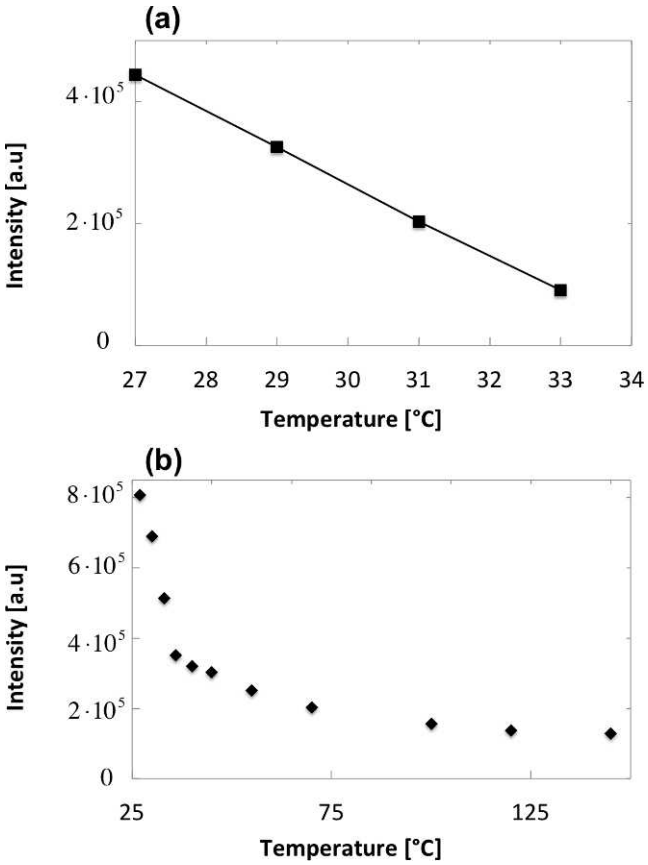

FIGURE 10. (**a**) Maximum intensity of peak E in Figure 9 as a function of temperature. The melt temperature for this peak is 34.34°C. The intensity of this peak decreases linearly with temperature. (**b**) Maximum intensity of peaks E+F in Figure 9 as a function of temperature.

bovine meibum to be structured as well. It is apparent that meibum is structured from a thick bulk-oil film down to films of several molecular layers in thickness.

In addition to the lamellar crystals identified in SAXS as melting by 37°C, scattering at wide angles (WAXS) demonstrates a broad peak that persists up to 145°C. The broad nature of this peak indicates that although lipid molecules are ordered, the spacing of that ordering is not conserved and there is a distribution of spacings. Such a distribution suggests that the lipids are in a bulk disordered phase.

Micrographs recorded from the polarized-light microscope (Olympus BX51; Olympus) indicate that the crystalline material in bovine meibum is anisotropic as it causes birefringence. The birefringence disappears when samples are heated past 37°C, the same temperature at which the SAXS shows disappearance of the last crystalline material. Thus, all structural evidence obtained in this work agrees that the crystalline material is lamellar in structure. The absence of birefringence above 37°C is consistent with the WAXS spectra indicating a disordered fluid phase.

Thermal analysis of bovine meibum with DSC corroborates the results of SAXS, WAXS, rheology, and light microscopy confirming phase transitions and their reversibility over the temperature range of 20 to 35°C. The transition region corresponds to the melting/crystallization of the three ordered lamellar phases identified by x-ray scattering. The two thermal peaks detected at 0 and 100°C, their disappearance on heating to 200°C or on desiccation, and their reappearance on water-vapor saturation strongly links them to absorbed water that melts and then evaporates during heating. The significant amount of water detected rejects possible sample contamination or adsorbed surface water. Because unstirred meibum reversibly absorbs and desorbs water when in contact with humidified air, dispersed droplets are unlikely. More likely, molecular domains of water may be present in the TFLL, but further research is needed to determine the state of water within the TFLL. The complete loss of meibum elasticity observed at 140°C (see Fig. 4a), is not detected in the DSC experiments, suggesting that it is not due to a first-order phase transition. The thermal peak at 125°C, which does not reappear after heating or on water-vapor saturation, apparently belongs to an unidentified, relatively low-molecular-weight organic compound.

In Figure 14, we propose an alternative schematic of the TFLL based on the experimental structural information gained here. The picture emerging from our study, and illustrated in Figure 14, is that of a viscoelastic, shear-thinning duplex fluid film covering the aqueous tear film that is thick enough to consist of two distinct interfaces: lipid/water and lipid/air separated by intervening bulk liquid. In addition to a plethora of lipid chemical molecules present, the TFLL also apparently contains protein[9,10] and water (not shown in Fig. 14). At physiologic temperature, 34 to 35°C, the bulk liquid is a suspension of lamellar crystallites (gray shading in Fig. 14) in a continuous fluid (orange shading in Fig. 14) and is highly viscoelastic and shear-thinning. The presence of lamellar crystals in both bulk samples and thin films of meibum[14,47] confirm that they are also present in the in vivo tear film. Asymmetric lamellar crystals added to oil mixtures in cosmetics and food emulsions are well known to impart structure reflected in material texture.[48–50] In fact, many of the lipids chemically identified in meibum, including polar lipids, wax esters, triglycerides, and fatty acids are known oil structurants.[50] The lamellar solids in meibum are minority components, yet they impart strong viscoelasticity. This result suggests that they are randomly oriented and highly asymmetric (e.g., needlelike). We have no evidence to support the picture in Figure 13 of the lipid layer as an ordered, stacked array of lamellar layers.

The solid lamellar particles (shown gray in Fig. 14) are dispersed in a continuous liquid phase (seen as orange in Fig. 14) that exhibits short-range order at physiologic temperature, but is overall disordered. We do not have definite evidence for the detailed molecular structure of the suspending, continuous liquid phase. However, above 37°C where all crystallites melt, this fluid is viscoelastic and non-Newtonian, although less so than with the crystalline particulates present. The different lamellar crystallites presented in Figure 14 refer to the lamellar phases found in bovine meibum. However, due to the similarity between the bulk structure of bovine and human meibum, the proposed model can describe the human TFLL with slight changes in the spacing of the lamellae.

Because hydrocarbons are not surface active at an oil/air interface, no significant segregation in either composition or molecular orientation is expected at the lipid/air interface of the tear-film lipid layer. Conversely, amphiphilic surfactantlike molecules, such as phospholipids, fatty acids, or omega-hydroxy acyl fatty acids, are expected to concentrate and orient at the water/lipid interface of the TFLL. Within a few layers, the molecular-orienting effect of the lipid/water interface is lost. As indicated in Figure 14, aqueous protein can also competitively adsorb at this interface and slowly unravel and irreversibly attach.[51–54] Penetration of aqueous protein into the bulk of the tear lipid layer (see Refs. 2, 26, 55, and 56 and Millar TJ and Mudgil P. *IOVS* 2005;46:ARVO E-Abstract 4418; see for instance Fig. 6 of Ref. 2) appears unlikely, as no favorable driving force is evident. Protein

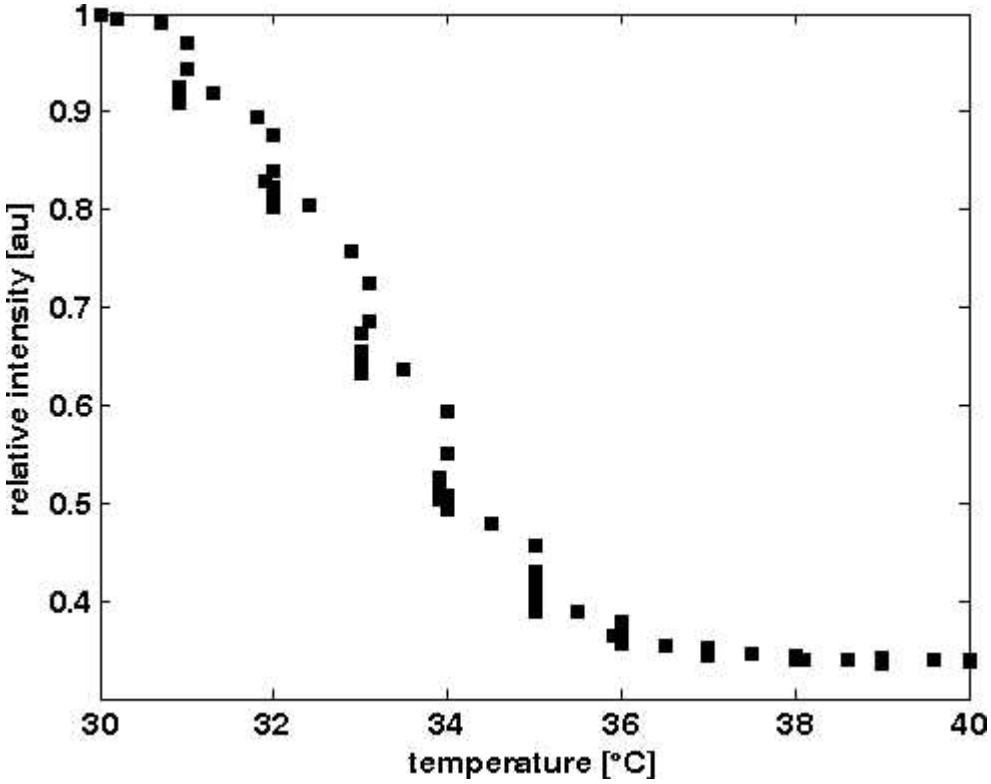

FIGURE 11. Birefringence melt curve for bovine meibum showing I/I_{max} of micrographs versus temperature.

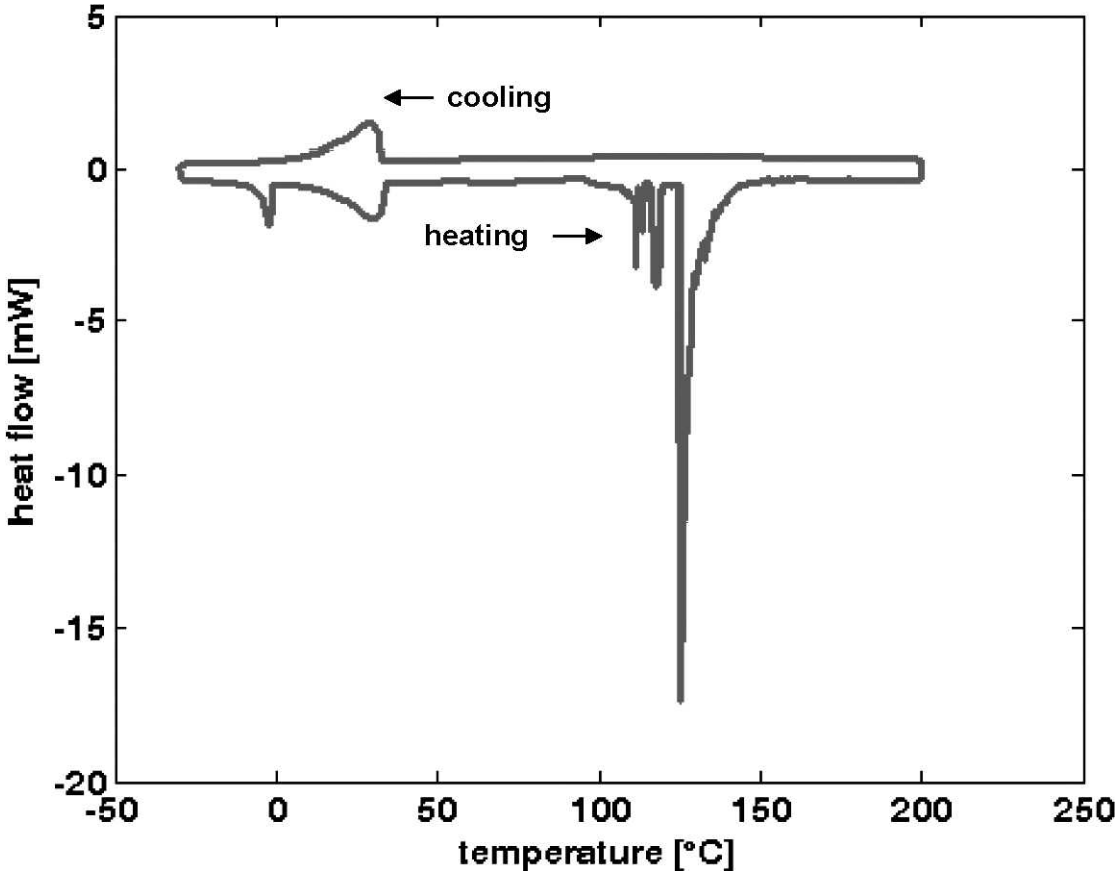

FIGURE 12. DSC heat flow versus temperature for bovine meibum collected from an individual animal. *Downward peaks* represent heat absorption by the sample (endothermic phase transitions) and *upward peaks* represent heat released from the sample (exothermic phase transitions). Sample mass is 9.5 mg. As indicated by the *horizontal arrows*, the *lower portion* of the curve corresponds to heating the sample from −30°C to 200°C and the *upper portion* to cooling from 200°C to −30°C.

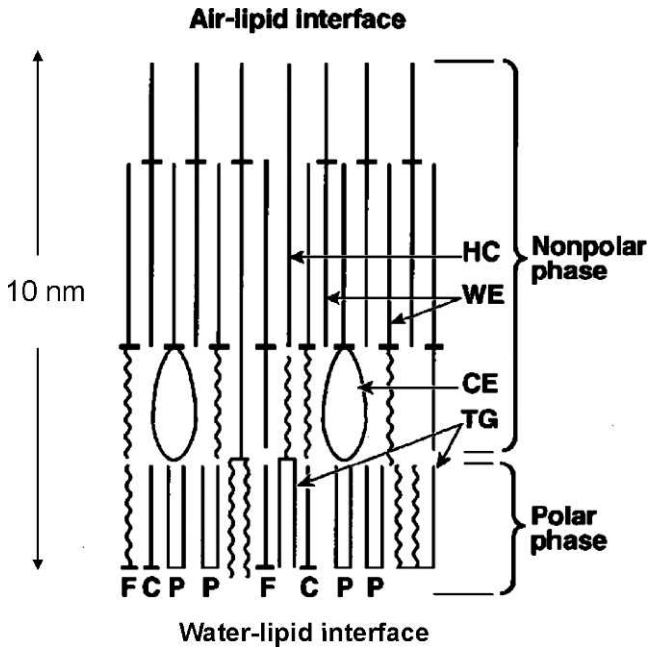

FIGURE 13. Lamellar structure of tear-film lipid layer. Symbol key: P, phospholipids; TG, triglycerides; WE, waxy esters; C, cerebrosides; HC, hydrocarbons; F, fatty acids (free); CE, cholesteryl esters. Modified and reprinted with permission from McCulley JP, Shine W. A compositional based model for the tear film lipid layer. *Trans Am Ophthalmol Soc*. 1997;95:79–93. Copyright 1997 American Ophthalmological Society.

observed in the chemical makeup of human meibum[9,10] might arise as detritus from the holocrine cells that produce meibum. However, protein within expelled meibum is likely to be partially denatured and not enzymatically active.[8]

The unique temperature dependence of the interfacial and bulk rheological properties of meibum is important to on-eye behavior. In a healthy eye, a smaller viscosity at body temperature facilitates expression from the glands and spreading of fresh lipid onto the tear-film surface. The TFLL is likely composed of both thick regions (~100 nm) and thinner regions away from the spreading front, possibly down to several monolayers. Thus, both bulk and interfacial rheology are pertinent. During spreading over the aqueous tear film, lipids cool and their bulk and interfacial elasticity increase. Increased elasticity may enhance the stability of the tear film protecting against rupture (i.e., formation of black spots). In the thinner regions of the lipid layer, dewetting of the lipid film may occur, resulting in lipid lenses interspersed in a monolayer or several-layer-thick oily film at the air/tear interface.[41,42] Lipid-layer breakup is detrimental because tear evaporation through the resulting thin monolayer regions is likely enhanced compared with that through the thicker regions of the lipid film. Cooling of the spreading lipid layer greatly increases its viscoelasticity, protecting against lipid-layer dewetting.

There is, thus, a delicate balance between lipid fluidity and structure necessary to enable uniform spreading over the tear film and also to resist dewetting of both the tear film and lipid layer itself. Accordingly, small changes in meibum melt temperature could detrimentally influence both lipid secretion and lipid-layer performance, raising important questions about the connection between meibum chemical composition and lipid-layer mechanical behavior on eye, especially for dry-eye and meibomian-gland disease (MGD) subjects. Our proposed lipid-layer structure in Figure 14 provides a new paradigm for

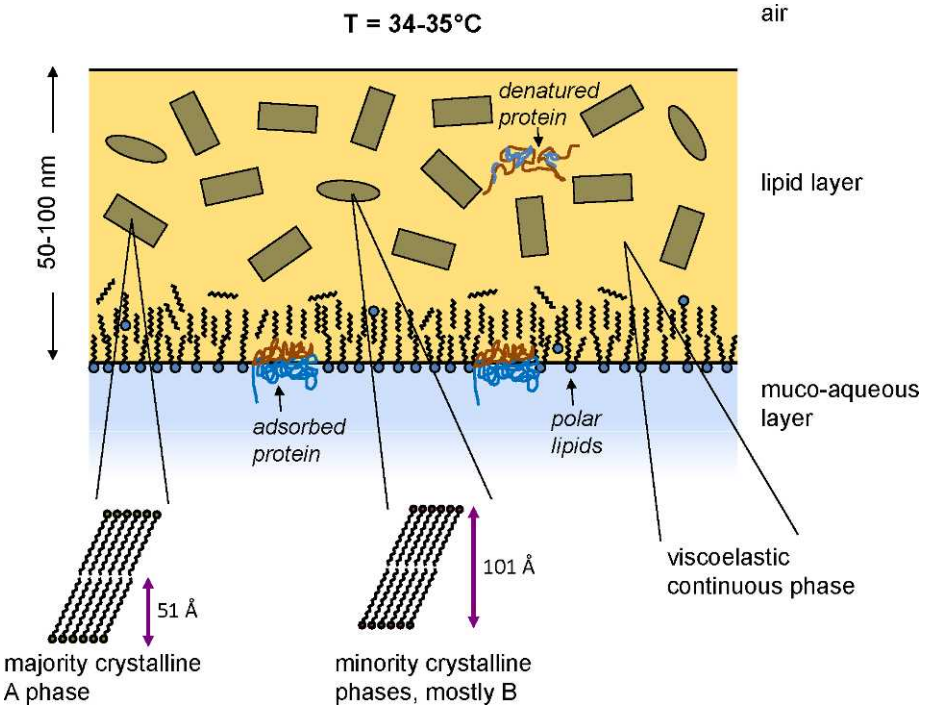

FIGURE 14. Proposed schematic of the tear-film lipid layer. At eye temperature, approximately 34 to 35°C, crystalline phases A to D are dispersed within an isotropic, viscoelastic continuous liquid (*orange shading*). Solid phase A (*gray rectangles*) is the majority crystalline phase. Crystallites are presumed highly asymmetric in shape. Polar lipids orient at the aqueous/lipid interface, but orientation does not persist deep into the bulk lipid layer. Proteins may also competitively adsorb at the aqueous/lipid and possibly intercalate. No specific orientation of lipid molecules is expected at the lipid/air interface. Water in the lipid layer is not shown. Drawing is not to scale.

understanding the human TFLL, but one that requires additional experimental verification and amplification.

Acknowledgments

We thank Michelle Senchyna for collection of human-meibum samples, Rachel Segalman at the University of California Berkeley for use of the DSC and microscope, and John Pople at the Stanford Linear Accelerator (SLAC) for help conducting SAXS and WAXS experiments. Portions of this research were carried out at the Stanford Synchrotron Radiation Lightsource, a Directorate of SLAC National Accelerator Laboratory and an Office of Science User Facility operated for the US Department of Energy Office of Science by Stanford University.

Supported in part by Alcon Research Ltd.

Disclosure: **L. Rosenfeld**, Alcon Research Ltd. (F); **C. Cerretani**, Alcon Research Ltd. (F); **D.L. Leiske**, Alcon Research Ltd. (F); **M.F. Toney**, None; **C.J. Radke**, Alcon Research Ltd. (F); **G.G. Fuller**, Alcon Research Ltd. (F)

References

1. King-Smith PE, Fink B, Hill R, Koelling K, Tiffany JM. The thickness of the tear film. *Curr Eye Res*. 2004;29:357–368.
2. Butovich IA, Millar TJ, Ham BM. Understanding and analyzing meibomian lipids—a review. *Curr Eye Res*. 2008;33:405–420.
3. Nagyova B, Tiffany JM. Components responsible for the surface tension of human tears. *Curr Eye Res*. 1999;19:4–11.
4. The definition and classification of dry eye disease: report of the Definition and Classification Subcommittee of the International Dry Eye Workshop (2007). *Ocul Surf*. 2007;5:75–92.
5. Butovich IA. Cholesteryl esters as a depot for very long chain fatty acids in human meibum. *J Lipid Res*. 2009;50:501–513.
6. Butovich IA, Uchiyama E, McCulley JP. Lipids of human meibum: mass-spectrometric analysis and structural elucidation. *J Lipid Res*. 2007;48:2220–2235.
7. Chen JZ, Green-Church KB, Nichols KK. Shotgun lipidomic analysis of human meibomian gland secretions with electrospray ionization tandem mass spectrometry. *Invest Ophthalmol Vis Sci*. 2010;51:6220–6231.
8. Green-Church KB, Butovich I, Willcox M, et al. The International Workshop on Meibomian Gland Dysfunction: report of the Subcommittee on Tear Film Lipids and Lipid-Protein Interactions in Health and Disease. *Invest Ophthalmol Vis Sci*. 2011;52:1979–1993.
9. Borchman D, Yappert MC, Foulks GN. Changes in human meibum lipid with meibomian gland dysfunction using principal component analysis. *Exp Eye Res*. 2010;91:246–256.
10. Tsai PS, Evans JE, Green KM, et al. Proteomic analysis of human meibomian gland secretions. *Br J Ophthalmol*. 2006; 90:372–377.
11. Bron AJ, Tiffany JM, Gouveia SM, Yokoi N, Voon LW. Functional aspects of the tear film lipid layer. *Exp Eye Res*. 2004;78:347–360.
12. Tiffany JM, Dart J. Normal and abnormal functions of the meibomian secretion. *R Soc Med Int Congr Symp Ser*. 1981; 40:1061–1064.
13. Borchman D, Foulks GN, Yappert MC, Ho DV. Temperature-induced conformational changes in human tear lipids hydrocarbon chains. *Biopolymers*. 2007;87:124–133.
14. Leiske DL, Leiske C, Leiske D, et al. Temperature-induced transitions in the structure and interfacial rheology of human meibum. *Biophys J*. 2012;102:369–376.
15. Leiske DL, Raju SR, Ketelson HA, Millar TJ, Fuller GG. The interfacial viscoelastic properties and structures of human and animal meibomian lipids. *Exp Eye Res*. 2010;90:598–604.
16. Nicolaides N, Kaitaranta JK, Rawdah TN, Macy JI, Boswell FM, Smith RE. Meibomian gland studies—comparison of steer and human lipids. *Invest Ophthalmol Vis Sci*. 1981;20:522–536.
17. Nicolaides N, Ruth EC. Unusual fatty-acids in the lipids of steer and human meibomian gland excreta. *Curr Eye Res*. 1982;2: 93–98.
18. Schein OD, Tielsch JM, Munoz B, Bandeen-Roche K, West S. Relation between signs and symptoms of dry eye in the elderly. A population-based perspective. *Ophthalmology*. 1997;104:1395–1401.
19. Brooks CF, Fuller GG, Frank CW, Robertson CR. An interfacial stress rheometer to study rheological transitions in monolayers at the air-water interface. *Langmuir*. 1999;15:2450–2459.
20. Reynaert S, Brooks CF, Moldenaers P, Vermant J, Fuller GG. Analysis of the magnetic rod interfacial stress rheometer. *J Rheol*. 2008;52:261–285.
21. Butovich IA. Lipidomics of human meibomian gland secretions: chemistry, biophysics, and physiological role of meibomian lipids. *Prog Lipid Res*. 2011;50:278–301.
22. Butovich IA, Wojtowicz JC, Molai M. Human tear film and meibum. Very long chain wax esters and (o-acyl)-omega-hydroxy fatty acids of meibum. *J Lipid Res*. 2009;50:2471–2485.
23. McCulley JP, Shine W. A compositional based model for the tear film lipid layer. *Trans Am Ophthalmol Soc*. 1997;95:79–93.
24. Tiffany JM. Individual variations in human meibomian lipid-composition. *Exp Eye Res*. 1978;27:289–300.
25. McCulley JP, Shine WE. The lipid layer: the outer surface of the ocular surface tear film. *Biosci Rep*. 2001;21:407–418.
26. Millar TJ, Tragoulias ST, Anderton PJ, et al. The surface activity of purified ocular mucin at the air-liquid interface and interactions with meibomian lipids. *Cornea*. 2006;25:91–100.
27. Tragoulias ST, Anderton PJ, Dennis GR, Miano F, Millar TJ. Surface pressure measurements of human tears and individual tear film components indicate that proteins are major contributors to the surface pressure. *Cornea*. 2005;24:189–200.
28. Butovich IA. The meibomian puzzle: combining pieces together. *Prog Retin Eye Res*. 2009;28:483–498.
29. Doane MG. An instrument for in vivo tear film interferometry. *Optom Vis Sci*. 1989;66:383–388.
30. Ehlers N. The precorneal film: biomicroscopical, histological and chemical investigations. *Acta Ophthalmol*. 1965;81:1–136.
31. Fatt I, Weissman BA. *Physiology of the Eye: An Introduction to the Vegetative Functions*. 2nd ed. Stoneham, MA: Butterworth-Heinemann; 1992.
32. Goto E, Dogru M, Kojima T, Tsubota K. Computer-synthesis of an interference color chart of human tear lipid layer, by a colorimetric approach. *Invest Ophthalmol Vis Sci*. 2003;44: 4693–4697.
33. Guillon J-P. Tear film photography and contact lens wear. *Journal of the British Contact Lens Association*. 1982;5:84–87.
34. Korb DR, Greiner JV, Glonek T, et al. Human and rabbit lipid layer and interference pattern observations. In: Sullivan DA, Dartt DA, Meneray MA, eds. *Lacrimal Gland, Tear Film, and Dry Eye Syndromes 2: Basic Science and Clinical relevance*. New York: Plenum Press; 1998:305–308.
35. McDonald JE. Surface phenomena of tear film. *Am J Ophthalmol*. 1969;67:56–64.
36. King-Smith PE, Hinel EA, Nichols JJ. Application of a novel interferometric method to investigate the relation between lipid layer thickness and tear film thinning. *Invest Ophthalmol Vis Sci*. 2010;51:2418–2423.
37. Harkins WD. A general thermodynamic theory of the spreading of liquids to form duplex films and of liquids or solids to form monolayers. *J Chem Phys*. 1941;9:552–568.

Investigative Ophthalmology & Visual Science

38. Heymann E, Yoffe A. The stability of multimolecular films of hydrocarbon oils, containing spreaders, on water surfaces. *Transactions of the Faraday Society*. 1942;38:408–417.
39. Holly FJ. Formation and rupture of the tear film. *Exp Eye Res*. 1973;15:515–525.
40. Holly FJ. Surface chemistry of tear film component analogs. *J Colloid Interface Sci*. 1974;49:221–231.
41. King-Smith PE, Nichols JJ, Braun RJ, Nichols KK. High resolution microscopy of the lipid layer of the tear film. *Ocul Surf*. 2011;9:197–211.
42. Millar TJ, King-Smith PE. Analysis of comparison of human meibomian lipid films and mixtures with cholesteryl esters in vitro films using high resolution color microscopy. *Invest Ophthalmol Vis Sci*. 2012;53:4710–4719.
43. Yokoi N, Yamada H, Mizukusa Y, et al. Rheology of tear film lipid layer spread in normal and aqueous tear-deficient dry eyes. *Invest Ophthalmol Vis Sci*. 2008;49:5319–5324.
44. Kim J, Conway A, Chauhan A. Extended delivery of ophthalmic drugs by silicone hydrogel contact lenses. *Biomaterials*. 2008;29:2259–2269.
45. Mudgil P, Millar TJ. Surfactant properties of human meibomian lipids. *Invest Ophthalmol Vis Sci*. 2011;52:1661–1670.
46. Stewart M, Stafford KJ, Dowling SK, Schaefer AL, Webster JR. Eye temperature and heart rate variability of calves disbudded with or without local anaesthetic. *Physiol Behav*. 2008;93:789–797.
47. Leiske DL, Miller CE, Rosenfeld L, et al. Molecular structure of interfacial human meibum films. *Langmuir*. 2012;28:11867–11874.
48. Floter E, Bot A. Developing products with modified fats. In: Williams C, Buttriss J, eds. *Improving Fat Content of Foods*. Cambridge: Woodhead Publishing; 2006;411–427.
49. Floter E, van Dujin G. Tran-free fat for use in foods. In: Gunstone F, ed. *Modifying Lipids for Food Use*. Cambridge: Woodhead Publishing; 2006;429–443.
50. Pernetti M, van Malssen KF, Floter E, Bot A. Structuring of edible oils by alternatives to crystalline fat. *Curr Opin Colloid Interface Sci*. 2007;12:221–231.
51. Beverung CJ, Radke CJ, Blanch HW. Protein adsorption at the oil/water interface: Characterization of adsorption kinetics by dynamic interfacial tension measurements. *Biophys Chem*. 1999;81:59–80.
52. Cascao Pereira LG, Hickel A, Radke CJ, Blanch HW. A kinetic model for enzyme interfacial activity and stability: Pa-hydroxynitrile lyase at the diisopropyl ether/water interface. *Biotechnol Bioeng*. 2002;78:595–605.
53. Hickel A, Radke CJ, Blanch HW. Hydroxynitrile lyase adsorption at liquid/liquid interfaces. *J Mol Catal B Enzym*. 1998;5:349–354.
54. Tupy MJ, Blanch HW, Radke CJ. Total internal reflection fluorescence spectrometer to study dynamic adsorption phenomena at liquid/liquid interfaces. *Ind Eng Chem Res*. 1998;37:3159–3168.
55. Miano F, Calcara M, Millar TJ, Enea V. Insertion of tear proteins into a meibomian lipids film. *Colloids Surf B Biointerfaces*. 2005;44:49–55.
56. Mudgil P, Torres M, Millar TJ. Adsorption of lysozyme to phospholipid and meibomian lipid monolayer films. *Colloids Surf B Biointerfaces*. 2006;48:128–137.

Investigative Ophthalmology & Visual Science